Cannabis and Cannabinoid Research
Volume 6, Number 4, 2021

DOI: 10.1089/can.2020.0046

The CB_1 Receptor Differentially Regulates IFN-γ Production *In Vitro* and in Experimental Autoimmune Encephalomyelitis

James M. Nichols and Barbara L.F. Kaplan*

Abstract

Introduction: Activation of the peripheral immune system and the infiltration of immune cells into the central nervous system are both key features of the experimental autoimmune encephalomyelitis (EAE) model. By exploring how the endocannabinoid system works to modulate this response, we can better understand how exogenous cannabinoids, such as THC, might be used to modulate the immune responses of multiple sclerosis patients.

Materials and Methods: In this study, we examined the role of the CB_1 receptor in IFN-γ and IL-17A production in the EAE model and *in vitro* stimulations of naive splenocytes using *Cnr1*$^{-/-}$ mice and wild-type (WT) littermates. We also introduce a novel method of scoring spinal cord histological sections to show the differences in disease severity between *Cnr1*$^{-/-}$ and WT mice with EAE.

Results: Clinical scores of *Cnr1*$^{-/-}$/EAE and WT/EAE mice showed more severe disease progression in *Cnr1*$^{-/-}$ mice, which was confirmed using our new histological scoring method. In the peripheral immune system, IFN-γ production by restimulated splenocytes from *Cnr1*$^{-/-}$/EAE mice, compared with WT/EAE mice, was increased and the primary source of IFN-γ was a $CD3^-$ cell population; however, IFN-γ production by *Cnr1*$^{-/-}$ splenocytes was decreased compared with WT splenocytes when the primary source of IFN-γ was $CD3^+$ T cells in cultures from naive mice stimulated by either anti-CD3/anti-CD28 antibodies or Staphylococcal superantigens.

Conclusion: These findings suggest a duality to the CB_1 receptor's effects on the peripheral immune response, which varies based on the specific cell types stimulated. Knowledge of the complex nature of a receptor is an important part of determining its potential usefulness as a therapeutic target, and these findings further define the role of CB_1 in IFN-γ responses.

Keywords: CB_1 receptor; experimental autoimmune encephalomyelitis; IFN-γ; multiple sclerosis

Introduction

Multiple sclerosis (MS) is a neurodegenerative autoimmune disease with a complex and incompletely understood etiology that affects millions of people worldwide, and more commonly affects women than men.[1–4] Current therapeutic measures used to treat MS have shown promise in reducing the severity of relapsing remitting MS, but most still fall short of preventing the long-term progression of disease seen in secondary and primary progressive MS.[2,5] As a result, research continues to be done into potential therapeutic targets for MS treatments.

The cannabinoid receptors, CB_1 and CB_2, are G protein-coupled receptors that signal predominantly via Gi/o. Activation of these receptors influences several intracellular pathways, including inhibition of cyclic AMP by adenylyl cyclase and activation of mitogen-activated protein kinases.[6] The ability of the cannabinoid receptors to act through these various pathways can cause a wide range of effects, including, but not limited to the following: hyperpolarization of neurons, inhibition of neurotransmitter release, changes in neuronal structure, modulation of intracellular calcium levels,

Department of Basic Sciences, College of Veterinary Medicine, Mississippi State University, Mississippi State, Mississippi, USA.
Portions of this work were previously presented:
The Role of CB_1 in Experimental Autoimmune Encephalomyelitis (EAE). American Association of Immunologists (AAI) Annual Meeting, San Diego, California, USA, May 2019.
The Role of CB_1 in Experimental Autoimmune Encephalomyelitis (EAE). Mississippi Academy of Science Meeting, Starkville, Mississippi, USA, July 2019.

*Address correspondence to: Barbara L.F. Kaplan, PhD, Department of Basic Sciences, College of Veterinary Medicine, Mississippi State University, 240 Wise Center Drive, Mississippi State, MS 39762, USA, E-mail: barbara.kaplan@msstate.edu

modulation of nitric oxide production, modulation of cytokine production, and increased migration of various immune cells. With this wide range of potential responses, it is obvious why the use of cannabinoids as treatment options is such a complex area of research.[6,7]

Experimental autoimmune encephalomyelitis (EAE) is a neuroinflammatory model commonly used to study the pathophysiology of MS, and although it does not provide a perfect replica of the clinical progression in humans, it has been critical for advancing MS therapies.[8] Studies that utilize this model often examine the IFN-γ and IL-17A cytokines, among other end-points, because of their association with Th_1 and Th_{17} cells, respectively, which have been shown to play an important role in the pathogenesis of EAE and MS.[9–15]

In the EAE model, CB_1 and CB_2 receptors have the potential to be both neuroprotective and anti-inflammatory[16,17]; however, it is unclear to what extent these two receptors are involved in regulation of the peripheral and neuroimmune responses. Previous studies of the CB_1 receptor have suggested that it is primarily responsible for the neuroprotective and antispasmodic affects seen with CB_1/CB_2 agonists in ABH mice with EAE, while the CB_2 receptor is primarily responsible for immunosuppressive effect of these compounds.[16–18] These results coincide with the fact that the CB_1 and CB_2 receptors are expressed predominately in the brain and peripheral immune system, respectively, but do not account for the putative effects of the CB_1 receptor in the peripheral immune system or CB_2 receptor in the central nervous system.[19–22]

In this study, we used C57BL/6 *Cnr1*$^{-/-}$ mice and wild-type (WT) littermates to examine the effects of the CB_1 receptor in EAE. C57BL/6 mice have been shown previously to be less susceptible to EAE than ABH mice, but generally have a more significant response to receptor deletions in the endocannabinoid system compared with ABH mice.[23] C57BL/6 mice have also been shown to be responsive to cannabinoid therapies in the EAE model.[9,24] Moreover, as phytocannabinoids, such as the THC:CBD mixture Sativex®, show increasing promise in clinical trials with MS patients as an antispasmodic,[25–29] it becomes more important to fully elucidate the mechanisms of these compounds and the receptors through which they act. In addition to exploring the effects of the CB_1 receptor in the peripheral and neuroimmune responses in EAE using various techniques, we developed a new histologic scoring system for the EAE model. Finally, we examined the role of CB_1 in naive splenocytes stimulated with anti-CD3/anti-CD28 or superantigen (SAg). Together, the results from this work represent an important step in understanding how CB_1 receptors influence IFN-γ and IL-17A production during inflammatory responses, and provide more insight into how therapies designed to target CB_1 receptors might alter peripheral and neuroimmune responses.

Materials and Methods

Reagents

Myelin oligodendrocyte glycoprotein (MOG) peptide (MEVGWYRSPFSRVVHLYRNGK) was purchased from Biosynthesis (Lewisville, TX), heat-killed *Mycobacterium tuberculosis* H37Ra (HKMT) was obtained from Difco/BD Biosciences (Detroit, MI), and complete Freund's adjuvant (CFA) was obtained from Sigma (St. Louis, MO). All other chemicals/reagents were obtained from Fisher Scientific unless otherwise noted.

Animals

The experiments performed in this study were approved by the Mississippi State University Institutional Animal Care and Use Committee (IACUC numbers 16-364, 17-342, and 19-273). Male and female *Cnr1*$^{-/-}$ and WT C57BL/6 littermates used in this study were bred at the Mississippi State University College of Veterinary Medicine after initial breeding pairs were obtained from the National Institutes of Health. EAE was induced in adult female mice ($\geq$8 weeks of age) and mice were housed three to five in a cage at a temperature (22°C$\pm$1°C)-, humidity (40–60%)-, and light (12-h light:12-h dark)-controlled room. Food and water were provided *ad libitum*, and as disease progressed, access to food and water was ensured through the use of longer sipper tubes and by placing food on the floor of the cages.

Induction and assessment of EAE

Female C57BL/6 mice were anesthetized using 3% isoflurane and immunized with CFA containing the $MOG_{35–55}$ peptide and HKMT. Each mouse was injected subcutaneously over the shoulders and hips with a total of 100 μL of CFA containing 100 μg of $MOG_{35–55}$ peptide and 500 μg of HKMT divided over four injection sites. Control mice received 100 μL saline (SAL) divided over four injection sites. These mice were then observed for an 18-day time period, and clinical scores were given based on the following scale: 0—Healthy; 0.5—Flaccid tail; 1—Hindlimb paresis; 1.5—Waddling gait; 2—Unable to prevent being placed in dorsal recumbency; 2.5—Hindlimb dragging;

3—Single hindlimb paralysis; 3.5—Single hindlimb paralysis with other hindlimb dragging; 4—Complete hindlimb paralysis; and 5—Moribund/involvement of forelimbs. Mice were never allowed to progress past the clinical score of 4 for animal welfare purposes. The clinical scores presented here represent the combined data of three independently performed studies.

Processing spinal columns

The entire spinal column was first isolated from each mouse and placed in 10% neutral buffered formalin for 1–2 weeks. They were then decalcified in 10% ethylenediaminetetraacetic acid (EDTA) for 15 days, with the EDTA solution being replenished every 5 days. Ten percent EDTA was made by diluting 0.5 M EDTA, pH 8 (Thermo Fisher) with distilled water, and adjusting the solution to pH 7.4. The spinal columns were cut into 0.5-cm sections beginning at approximately the T7 vertebrae using a razor blade and a premarked clear plastic culture plate to make sure the cuts were the same for each mouse. Each 0.5-cm section was then embedded in a cranial to caudal orientation within a paraffin wax block to ensure 0.5-cm spacing between adjacent tissue sections (Fig. 1A, C). This method was developed to ensure consistent spacing between sections regardless of the number of times the block is cut.

Histologic scoring

To analyze neuroinflammation within the spinal cord, a new scoring system was developed to account for variations in lesion size, location along the spinal cord, and location within a section associated with the EAE model. We first accounted for lesion size by assigning a number value to each lesion based on the number of cells within the lesion: 0 = 0 to 10 cells; 1 = 10 to 100 cells; 2 = 100 to 200 cells; and 3 ≥ 200 cells. Next, we accounted for location of the lesion along the spinal cord by using the sectioning method described above to obtain six sections at equal intervals along the spinal cord. Finally, we accounted for location within a section by dividing the sections into quadrants: left dorsal, right dorsal, left ventral, and right ventral (Fig. 1B). In each of these quadrants, we found the largest lesion and counted the number of cells within the lesion to obtain a score for that quadrant, and the four scores for a section were totaled to obtain a section score that could further be totaled with the other section scores to obtain a histological score for each mouse. Of the six sections obtained, hematoxylin and eosin (H&E) stains of the first five sections of spinal cord from each histologic preparation were used to generate histologic scores for each mouse, and analysis was performed to compare section scores between groups. Spinal cords were sectioned at 5 μm for H&E staining. Figure 1D shows an example of a lesion used to obtain a quadrant score. Microscopic images were captured using a Lumenera Digital Camera and Infinity Analyze Software. Scoring and lesion area measurements were done with ImageJ software.

Ex vivo restimulation

Splenocytes were isolated 18 days after initiation of disease by pressing the splenic tissue through a 70 μm filter, and 20×10^6 cells were seeded into a six-well plate in 4 mL of 1 × RPMI supplemented with 5% bovine calf serum (HyClone, Logan, UT), 1% penicillin/streptomycin (Gibco, Gaithersburg, MD), and 50 μM 2-mercaptoethanol (2-ME; Gibco). Cultures were restimulated with 50 μg/mL of MOG_{35-55} peptide and incubated at 37°C for 72 h, at which time the supernatants were removed for analysis by enzyme-linked immunosorbent assay (ELISA) and cells were analyzed by flow cytometry.

In vitro anti-CD3/anti-CD28 and *Staphylococcus aureus* SAg stimulation

Plates (48-well) were precoated with 200 μL of anti-CD3 antibody (BioLegend Clone 145-2C11) diluted in sterile phosphate-buffered saline (PBS) at 1 μg/mL (1:1000) or 0.5 μg/mL (1:2000) for 1 h at 37°C before culture. Next, the wells were rinsed 3 × with PBS, and the anti-CD28 antibody (BioLegend Clone 37.51) was added to the wells immediately before seeding 1×10^6 naive splenocytes isolated from male and female WT or *Cnr1*$^{-/-}$ mice in 1 mL of RPMI supplemented with 5% bovine calf serum, 1% penicillin/streptomycin, and 50 μM 2-ME. The final concentrations of anti-CD28 antibody were 1 μg/mL (1:1000) or 0.5 μg/mL (1:2000). Other wells were treated with 1 μg of staphylococcal enterotoxin M (SEM), 5 μg of SEM, or received no treatment. SEM was chosen for these experiments based on preliminary experiments, which showed consistent stimulation of T cells from C57BL/6 mice. These cultures were then incubated at 37°C for 2 or 3 days, and stained for flow cytometry as described below. Supernatants from these cultures were taken for IFN-γ ELISA.

Enzyme-linked immunosorbent assay

Immulon 4 HBX flat-bottomed plates were coated with purified mouse IL-17A (BioLegend Clone TC11-

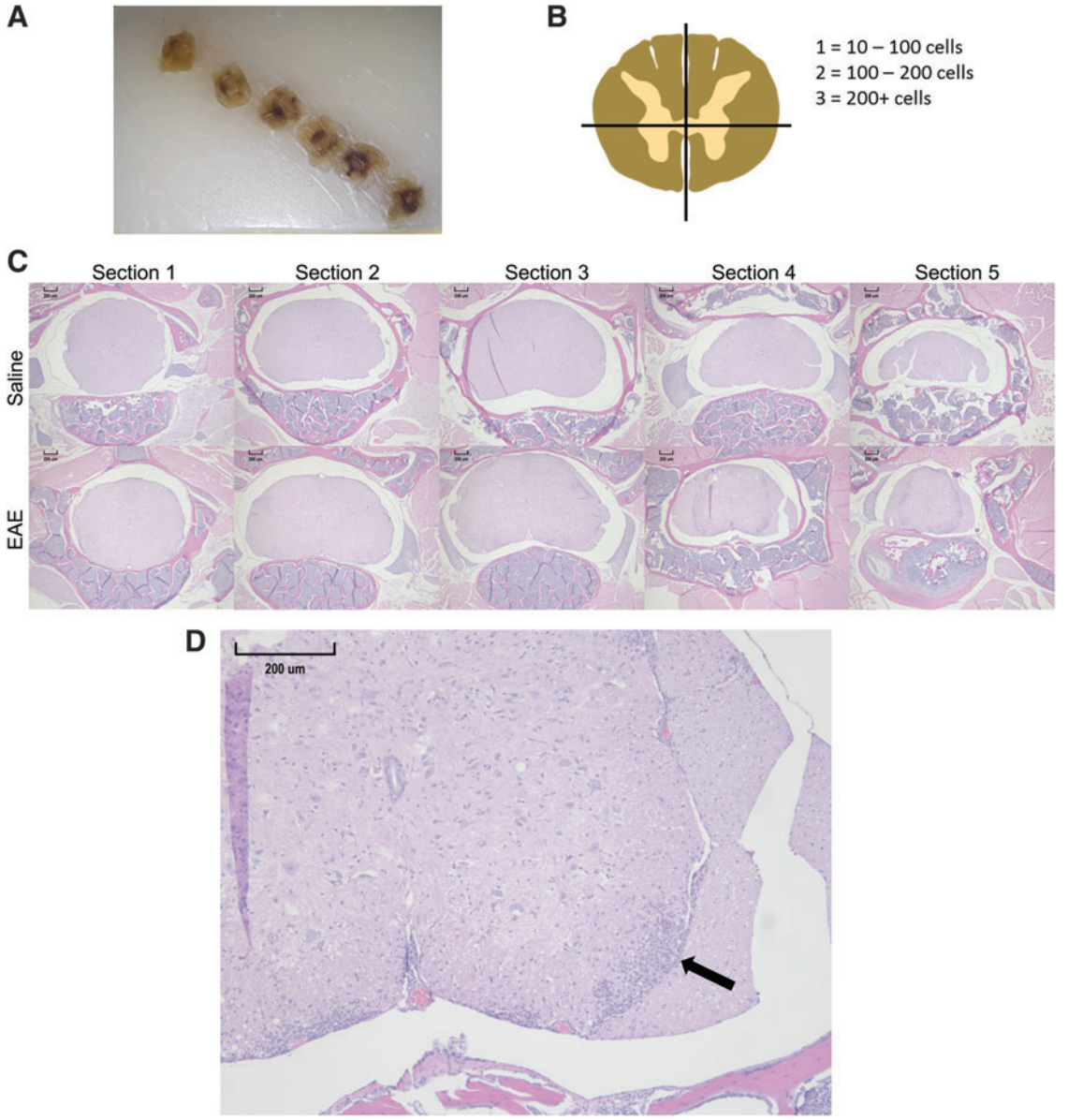

FIG. 1. Histologic scoring system. The spinal column for each mouse was sectioned into six-0.5 cm sections and placed in paraffin wax blocks so that the cranial aspect of each section would be cut first **(A)**. Then each quadrant of the first five sections was given a score based on the number of cells found within the largest lesion in each quarter of the spinal cord **(B)**. Representative 40× magnification hematoxylin and eosin images of the first five sections from a WT/SAL mouse and a *Cnr1*$^{-/-}$/EAE mouse are shown **(C)**. A 100× magnification of section 4 in the EAE mouse from **(C)** is depicted to show a typical lesion (arrow) in the right ventral quadrant of the spinal cord **(D)**. EAE, experimental autoimmune encephalomyelitis; SAL, saline; WT, wild type. Color images are available online.

18H10.1) or IFN-γ (BioLegend Clone AN-18) antibodies by adding 100 μL of coating buffer (4.2 g of $NaHCO_3$ in 500 mL of DI water) containing the desired antibody at a 1:500 dilution, and incubating the plate overnight at 4°C. The next day the plates were rinsed with PBS containing 0.05% Tween 20 (PBST), blocked with 3% bovine serum albumin (BSA)-PBS for 1 h at room temperature (RT), and rinsed again with PBST. Serial dilutions of recombinant IL-17A (BioLegend) or IFN-γ (BioLegend) standards (8000–7.8 pg/mL) and samples were pipetted into their designated wells. These included supernatants from the *ex vivo* MOG_{35-55} restimulation of splenocytes from EAE mice, serum from EAE mice, or supernatants from the *in vitro* anti-CD3/anti-CD28 and SEM stimulations. Various dilutions (1:10, 1:100, and 1:500) of each sample were also placed in ELISA plates and 3% BSA-PBS was used as a blank control. These were allowed to incubate in the ELISA plates for 1 h at RT, and the plates were rinsed with PBST. One hundred microliters of biotinylated IL-17A (BioLegend Clone TC11-8H4) or biotinylated IFN-γ (BioLegend Clone R4-6A2) antibodies in 3% BSA-PBS at a 1:500 dilution was added to their respective plates and incubated for 1 h at RT, and the plates were rinsed with PBST. After incubation with the biotinylated antibodies, the plates were rinsed with PBST and 100 μL of horseradish peroxidase (HRP)-Avidin in 3% BSA-PBS at a 1:500 dilution was added to each well and incubated for 1 h at RT. The plates were rinsed again with PBST and the tetramethylbenzidine substrate (BioLegend) was added and allowed to incubate in the dark at RT until a color change was seen in the lowest standard (7.8 pg/mL). At that time, 100 μL of 2 N H_2SO_4 was added to stop the reaction, and optical density was measured at 450 nm.

Flow cytometry

Cells from an *ex vivo* MOG_{35-55} restimulation of splenocytes from EAE mice and an *in vitro* anti-CD3/anti-CD28 and SEM stimulation were analyzed by flow cytometry in addition to ELISA performed on supernatants from these cultures. During the last 4 h of culture, cells were treated with brefeldin A to prevent further excretion of cytokines. Cells were then rinsed two times with PBS before staining with 0.1 μL of Zombie Near Infrared Fixable Viability Dye (NIR FVD; BioLegend) in 50 μL of PBS for 30 min at 4°C. NIR FVD was removed by rinsing twice with PBS, and 0.5 μL of Fc Block (purified mouse CD16/CD32; BD Biosciences, Billerica, MA) was added in 50 μL of flow cytometry media (FCM; 1 × Hank's buffered saline solution/1% BSA) 10 min before the addition of extracellular antibodies. A total of 0.3 μL each of CD4-PE (BioLegend Clone RM4-4), CD8α-PE/Cy7 (BioLegend Clone 53-6.7), and CD3-FITC (BD Bioscience Clone 145-2C11) antibodies in 50 μL was added to each sample and allowed to incubate for 30 min at RT. Cells were rinsed twice with FCM and fixed with BD Cytofix (BD Biosciences) for 15 min at RT. Cells were then rinsed once with FCM and once with BD perm/wash buffer (BD Biosciences) before the addition of 0.5 μL of IFN-γ-antigen presenting cell (APC; BioLegend Clone XMG1.2) in 50 μL of BD perm/wash buffer. The cells were incubated overnight at 4°C, rinsed with FCM, resuspended in 200 μL of FCM, and analyzed using an ACEA Novocyte flow cytometer (ACEA Biosciences, San Diego, CA).

Statistical analyses

All statistical analyses were done with GraphPad Prism 7 software. Histologic scores for each spinal cord section were analyzed using the Mann–Whitney U-test to compare between groups. ELISAs and area under the curve (AUC) for clinical progression were analyzed using two-way analysis of variance (ANOVA). Transformed percentages obtained from flow cytometry analysis were also analyzed using two-way ANOVA. Sidak's *post hoc* test was used to identify differences between groups following the two-way ANOVA. Graphical rerepresentations of results are mean ± SD.

Results

EAE was more severe in *Cnr1*$^{-/-}$ mice

By analyzing average AUC for each group of mice, we found that *Cnr1*$^{-/-}$ mice with EAE ($n = 12$) had significantly higher levels of disease over the 18-day timecourse compared with their WT littermates ($n = 14$) (Fig. 2A). SAL-treated *Cnr1*$^{-/-}$ ($n = 13$) and WT ($n = 13$) mice had no clinical disease. Figure 2B shows the progression of clinical disease during the 18-day timecourse.

Immune cell infiltration into spinal cords was higher in *Cnr1*$^{-/-}$ mice

Using our novel histologic scoring system as described in the Materials and Methods, histologic scores were totaled and analyzed for each of the five sections of spinal cord from each mouse. This analysis revealed that *Cnr1*$^{-/-}$ mice with EAE had significantly higher levels of cellular infiltration compared with their WT littermates in sections 2–4, while the first and fifth spinal

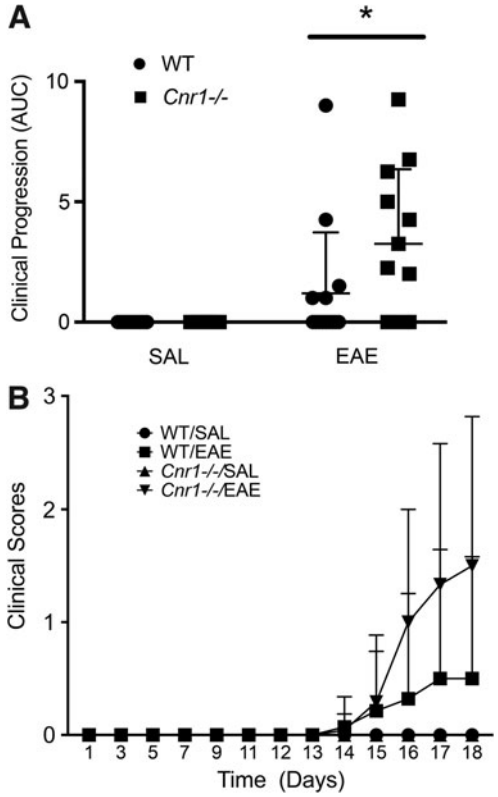

FIG. 2. Differences in clinical EAE between *Cnr1*$^{-/-}$ and WT littermates. Clinical scores for WT/SAL ($n=13$), WT/EAE ($n=14$), *Cnr1*$^{-/-}$/SAL ($n=13$), and *Cnr1*$^{-/-}$/EAE ($n=12$) mice were recorded over the 18-day timecourse of disease. Average AUC was then calculated for each experimental group and analyzed using a two-way ANOVA followed by Sidak's *post hoc* test **(A)**. The clinical scores were also graphed over time to show clinical progression for each group **(B)**. Analysis of the average AUC for disease progression of each group showed a statistically significant difference between the *Cnr1*$^{-/-}$/EAE mice and WT mice. Error bars represent the SD for each group (only top error bars are shown). *$p<0.05$ difference between WT and *Cnr1*$^{-/-}$ in EAE. ANOVA, analysis of variance; AUC, area under the curve.

cord section showed only a modest difference between these two groups (Fig. 3A). No infiltration was seen in any of the SAL mice examined. To validate this new scoring system, a total histological score was obtained for each mouse by adding the five section scores together, and the correlation between total histologic score and clinical score on day 18 was analyzed (Fig. 3B). Total lesion area was also tabulated for each mouse over the five sections, and then correlated to the clinical score to determine if lesion area would be a more representative measurement than our histologic scoring system (Fig. 3C). When section scores were totaled for each mouse and compared with clinical score at the day 18 time point, the histologic scores showed a high level of correlation to clinical scores ($r^2=0.7171$) (Fig. 3B). A similar level of correlation was found between the total lesion area and clinical score for each mouse ($r^2=0.7563$) (Fig. 3C).

IFN-γ production is differentially regulated in *Cnr1*$^{-/-}$ splenocytes depending on the method of stimulation

MOG$_{35-55}$ *ex vivo* restimulation. Analysis of IFN-γ and IL-17A in serum taken on day 18 and supernatants from *ex vivo* restimulated splenocytes showed that production of IFN-γ was significantly higher in restimulated cells from *Cnr1*$^{-/-}$/EAE mice compared with WT/EAE mice (Fig. 4A). However, no difference was seen with serum IFN-γ, serum IL-17A, or supernatant IL-17A (Fig. 4B–D).

Anti-CD3/anti-CD28 and SEM *in vitro* stimulation. To further investigate the T cell IFN-γ response of the *Cnr1*$^{-/-}$ mice, naive splenocytes were cultured for 2 or 3 days in the presence of anti-CD3/anti-CD28 antibodies or SEM, and IFN-γ was measured in the supernatants of these cultures by ELISA. In these experiments, both male and female mice were used to examine potential sex differences in the effects of CB$_1$ receptor deletion on IFN-γ production. For both male and female mice, the IFN-γ response in WT splenocytes stimulated with anti-CD3/anti-CD28 antibodies was significantly higher than that from *Cnr1*$^{-/-}$ mice at two different concentrations. Interestingly, while SEM-treated splenocytes showed a similar trend to the anti-CD3/anti-CD28-treated splenocytes, the differences observed between WT and *Cnr1*$^{-/-}$ mice did not reach the same level of significance seen with anti-CD3/anti-CD28 stimulation (Fig. 5A–D).

Identification of cell types producing IFN-γ in response to different stimuli

We used flow cytometry to identify whether the differential regulation of IFN-γ in the absence of CB$_1$ in

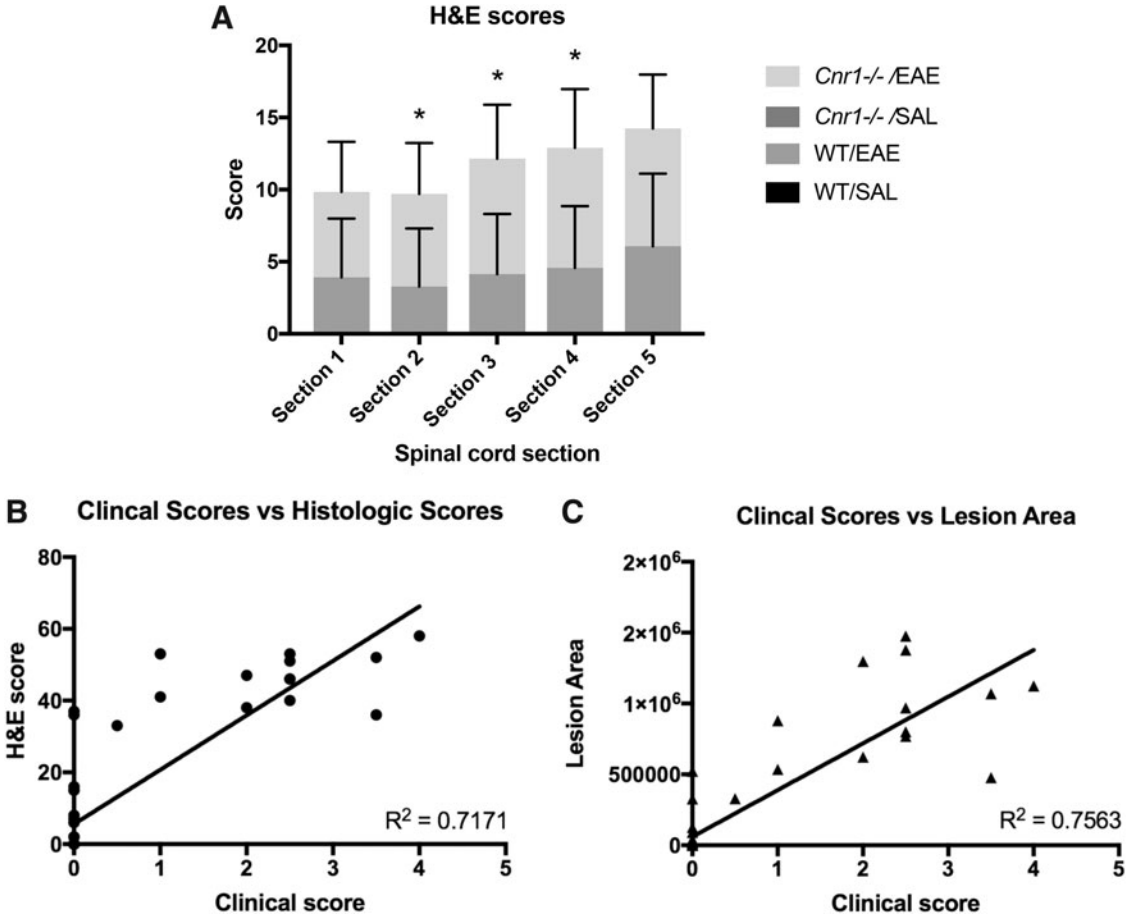

FIG. 3. Histologic scoring. Histologic scores using our novel scoring system were determined on spinal cords for WT/SAL ($n = 13$), WT/EAE ($n = 14$), $Cnr1^{-/-}$/SAL ($n = 13$), and $Cnr1^{-/-}$/EAE ($n = 12$) mice **(A)**. No infiltration was seen in any of the SAL mice examined, so scores for $Cnr1^{-/-}$/SAL and WT/SAL are all 0. Histologic scores for each spinal cord section were analyzed using the Mann–Whitney U-test to compare between groups. To validate this method of scoring, the histologic scores were correlated to the clinical scores for each mouse **(B)**. Lesion area for each mouse was also tabulated by finding the lesion area for each of the five spinal cord sections and adding them together, and then, this area was correlated to the clinical score for each mouse to determine if the lesion area was more representative of clinical disease **(C)**. Error bars represent the SD for each group. $^*p < 0.05$ difference between WT and $Cnr1^{-/-}$ in EAE.

ex vivo restimulated cells from EAE mice or *in vitro* stimulated cells from naive mice was due to distinct cell populations. For these analyses, we utilized only the 3-day anti-CD3/anti-CD28-stimulated cells from female splenocytes to allow a direct comparison with the MOG_{35-55}-restimulated cells in female splenocytes from EAE mice, which were also stimulated for 3 days. For both *ex vivo* restimulations and *in vitro* stimulations, live lymphocytes were gated first based on the NIR FVD stain, and then on the forward scatter (FSC) and side scatter (SSC) characteristics, which are commonly used to approximate size and granularity of lymphocytes, respectively. IFN-γ producing cells were then separated based on CD4 and/or CD8 expression. Cells that were negative for both CD4 and CD8 were analyzed further for CD3 expression (Figs. 6A and 7A).

MOG_{35-55} *ex vivo* restimulation. Analysis of the percentage of IFN-γ producing cells within the *ex vivo* restimulated splenocytes from EAE mice by flow

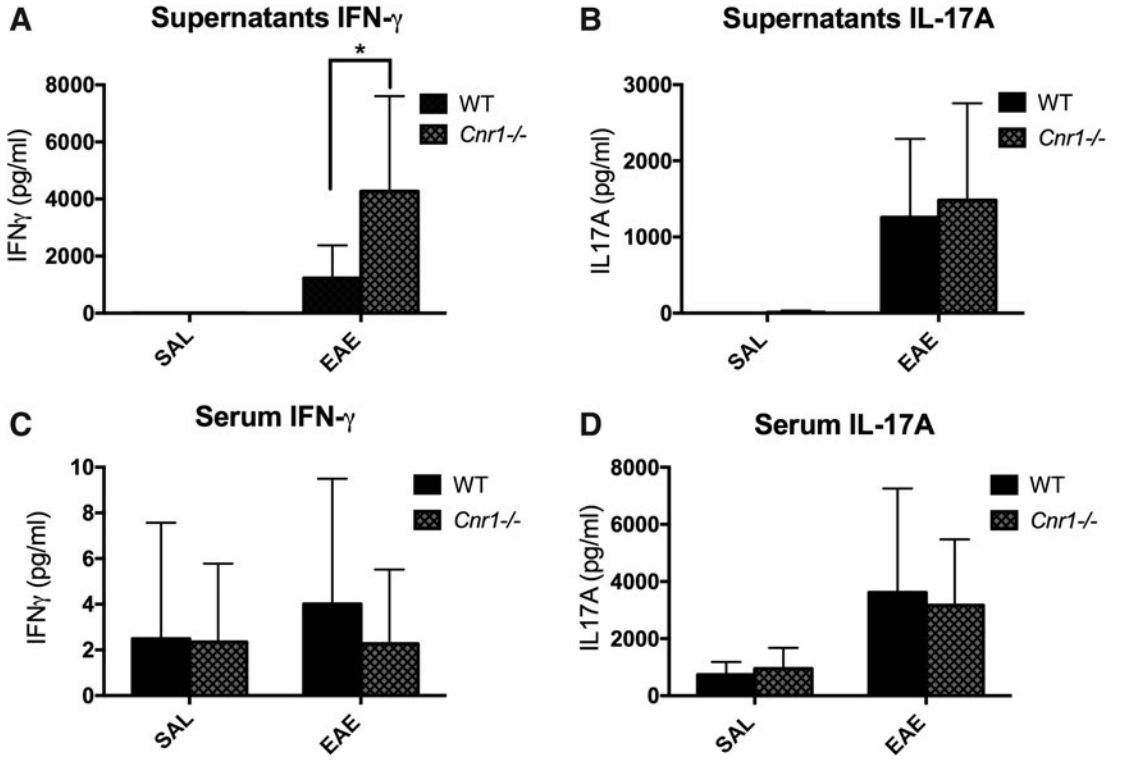

FIG. 4. IFN-γ and IL-17A in serum and $MOG_{35–55}$ restimulation cultures. Splenocytes were harvested from EAE and SAL control mice restimulated with $MOG_{35–55}$ peptide for 3 days. The supernatants from these cultures were then tested by ELISA for concentrations of IFN-γ (WT/SAL [$n=11$], WT/EAE [$n=11$], *Cnr1*$^{-/-}$/SAL [$n=11$], and *Cnr1*$^{-/-}$/EAE [$n=12$]), **(A)** and IL-17A (WT/SAL [$n=11$], WT/EAE [$n=14$], *Cnr1*$^{-/-}$/SAL [$n=11$], and *Cnr1*$^{-/-}$/EAE [$n=12$]) **(B)**. Serum was also taken from each mouse at the time of necropsy and tested by ELISA for concentrations of IFN-γ (WT/SAL [$n=13$], WT/EAE [$n=13$], *Cnr1*$^{-/-}$/SAL [$n=12$], and *Cnr1*$^{-/-}$/EAE [$n=10$]), **(C)** and IL-17A (WT/SAL [$n=10$], WT/EAE [$n=14$], *Cnr1*$^{-/-}$/SAL [$n=11$], and *Cnr1*$^{-/-}$/EAE [$n=12$]) **(D)**. Statistical analysis was performed using two-way ANOVA followed by Sidak's *post hoc* test. Bars represent the mean ± SD for each group. *$p<0.05$ difference between WT and *Cnr1*$^{-/-}$ in EAE. ELISA, enzyme-linked immunosorbent assay; MOG, myelin oligodendrocyte glycoprotein.

cytometry revealed no significant differences between the *Cnr1*$^{-/-}$ mice and WT littermates. However, it did show the primary source of IFN-γ to be a $CD3^-CD4^-CD8^-$ cell population (Fig. 6B).

Anti-CD3/anti-CD28 and SEM *in vitro* stimulation. Analysis of the percentage of IFN-γ producing cells within the *in vitro* stimulated splenocytes by flow cytometry revealed a significantly higher percentage of $CD8^+$IFN-γ^+ T cells in the anti-CD3/anti-CD28-stimulated WT cells compared with the *Cnr1*$^{-/-}$ cells. In contrast to the *ex vivo* restimulated splenocytes from EAE mice, the $CD3^+$ population played a large role in IFN-γ production *in vitro* (Fig. 7B).

Discussion

The purpose of this study was to examine the role of the CB_1 receptor in the EAE model, with a focus on differences in the peripheral immune and neuroimmune responses between *Cnr1*$^{-/-}$ mice and WT littermates. Our results showed that *Cnr1*$^{-/-}$ C57BL/6 mice had higher levels of clinical disease compared with their WT littermates. These results are slightly different than those previously reported by other laboratories using ABH *Cnr1*$^{-/-}$ mice. In one previous study, the authors found that ABH *Cnr1*$^{-/-}$ mice had similar levels of disease onset, incidence, and severity, but exhibited less of an ability to recover from paralytic episodes compared with WT mice, which suggested more

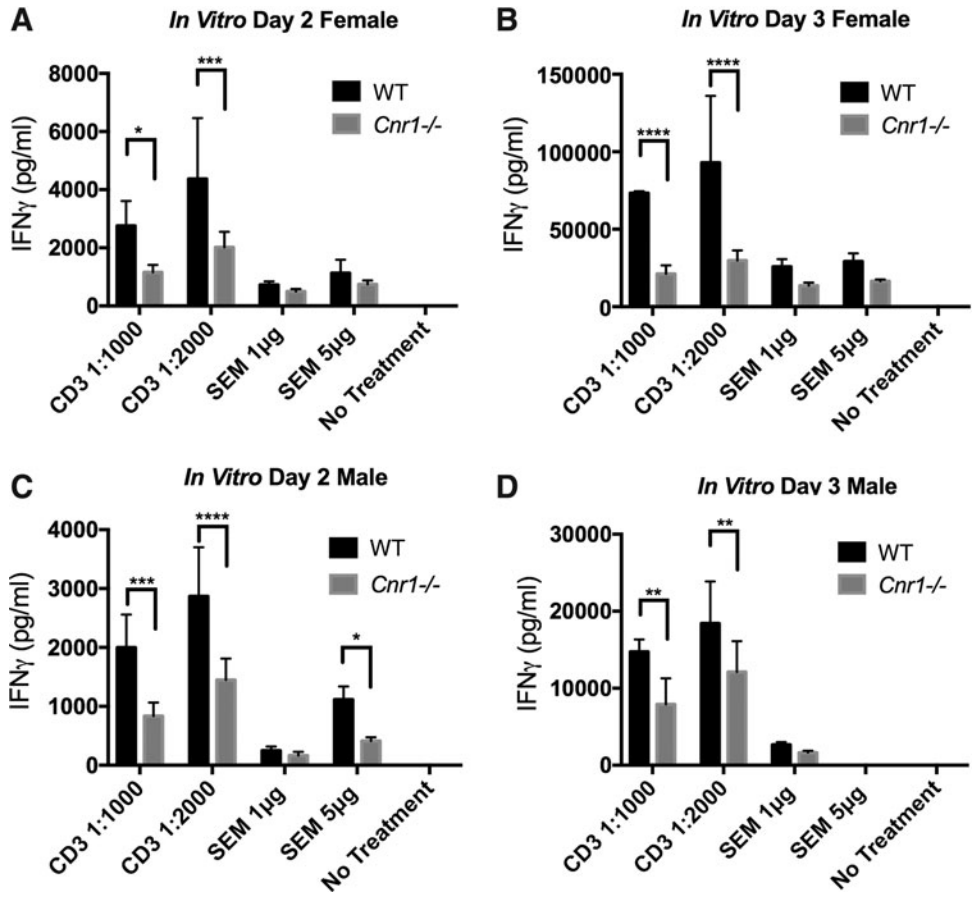

FIG. 5. Anti-CD3/anti-CD28 and SEM stimulation of naive T cells. Splenocytes were harvested from naive female and male WT and *Cnr1*$^{-/-}$ mice and stimulated with either anti-CD3/anti-CD28 antibodies or SEM superantigen for 2 or 3 days before IFN-γ concentrations within the supernatants were analyzed by ELISA **(A–D)**. Bars represent the mean ± SD from quadruplicate cultures. Statistical analysis was performed using two-way ANOVA followed by Sidak's *post hoc* test *$p < 0.05$, **$p < 0.01$, ***$p < 0.001$, ****$p < 0.0001$ differences between WT and *Cnr1*$^{-/-}$. Experiments are representative of two separate experiments performed in both female and male mice (no sex differences were noted). SEM, staphylococcal enterotoxin M.

axonal degradation in the *Cnr1*$^{-/-}$ mice.[16] In another study, CB_1-deficient mice only showed a higher level of disease when THC was used to treat the mice. The assumption in this latter study was that the CB_1 receptor did not play a role in suppressing disease in the steady state, but was important in cannabinoid therapies.[17] The differences seen between our results and those seen in the ABH mice might be due to a strain difference in the endocannabinoid system. More specifically, since neither of the previous studies in ABH mice showed the higher level of disease severity in *Cnr1*$^{-/-}$ mice that we show here, and the latter study showed differences in clinical disease only upon activation of the CB_1 receptor with THC, there may be higher levels of endocannabinoids or higher sensitivity of the CB_1 receptor to endocannabinoids in C57BL/6 mice compared with ABH mice. This would explain why we saw differences in disease severity without the use of exogenous cannabinoids. This is supported by a previous study using C57BL/6 mice in the EAE model, which found that mice treated with SR141716, a CB_1 receptor antagonist, developed EAE more rapidly than vehicle-treated mice, which resembles the differences in EAE that we found in our studies.[30] Additional work done by Sisay et al. has shown that there are differences in the immune responses between the

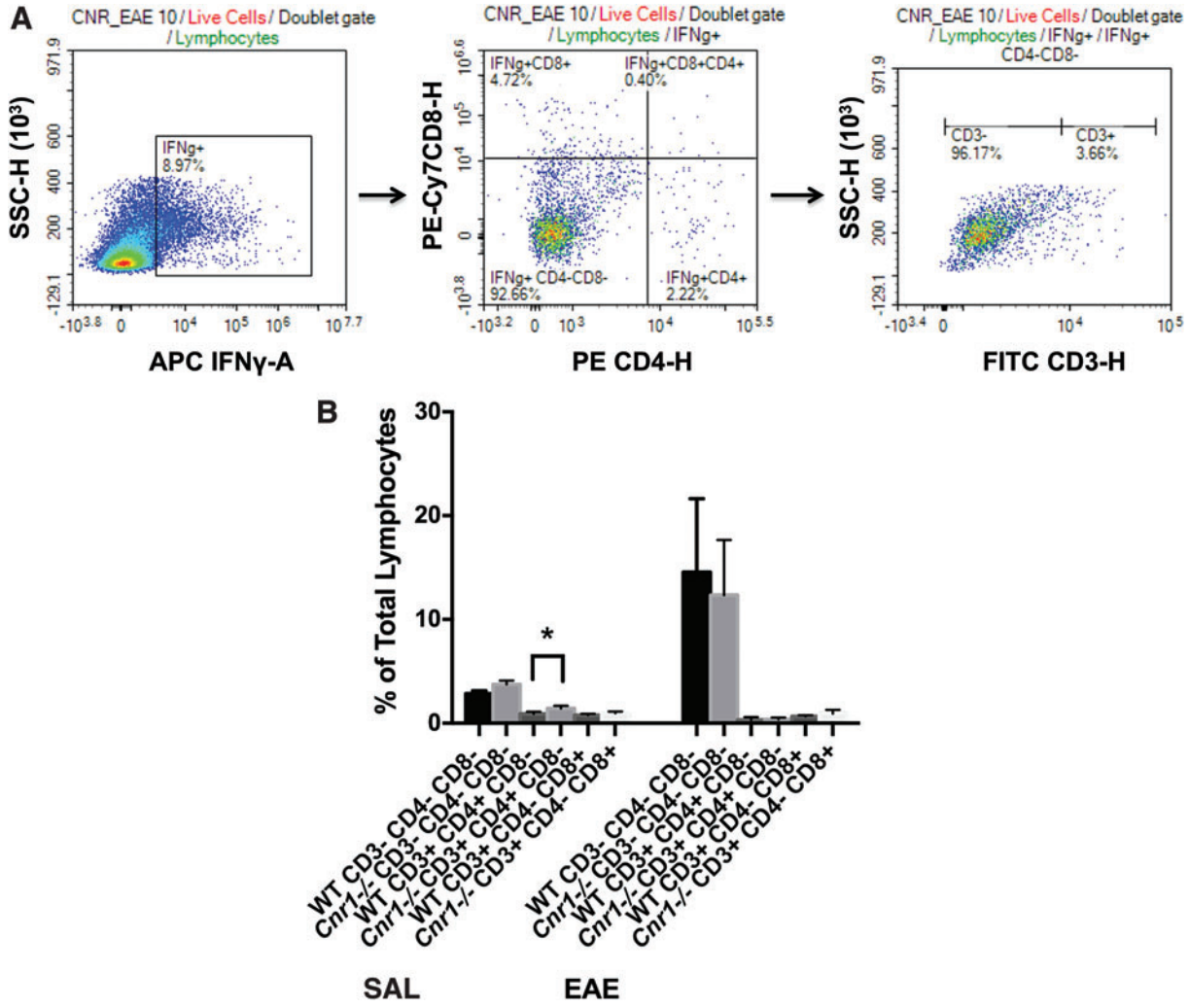

FIG. 6. Analysis of IFN-γ production in MOG_{35-55}-restimulated splenocytes by flow cytometry. IFN-γ production was analyzed by flow cytometry in the *ex vivo* MOG_{35-55}-restimulated splenocytes of WT/SAL ($n=5$), WT/EAE ($n=6$), *Cnr1*$^{-/-}$/SAL ($n=5$), and *Cnr1*$^{-/-}$/EAE ($n=5$) mice. IFN-γ producing cells were subdivided based on their CD4, CD8, and CD3 expression by first isolating IFN-γ producing lymphocytes, then determining the expression of CD4 and CD8 on these cells, and finally determining the expression of CD3 within the T cell subpopulations **(A)**. Analysis of various cell types revealed no significant differences between *Cnr1*$^{-/-}$/EAE and WT/EAE mice. A significantly higher percentage of $CD3^+CD4^+CD8^-$ cells was seen in *Cnr1*$^{-/-}$/SAL mice compared with WT/SAL mice. In addition, in these experiments, $CD3^-$ cells appear to be the predominant source of IFN-γ **(B)**. Statistical analysis was performed using two-way ANOVA followed by Sidak's *post hoc* test. Bars represent the mean ± SD for each group of mice. *$p<0.05$ difference between WT and *Cnr1*$^{-/-}$. Color images are available online.

responses of C57BL6 mice and ABH mice when the endocannabinoid system is modified within the context of the EAE model. This study examined the effects of multiple components of the endocannabinoid system, including the GPR55, TRPV1, CB1, and CB2 receptors, and their findings suggest that in ABH mice, these receptors played less of a role in immunomodulation than in C57BL6 mice.[23]

To confirm the results of our clinical scoring, a new histologic scoring system was developed to determine

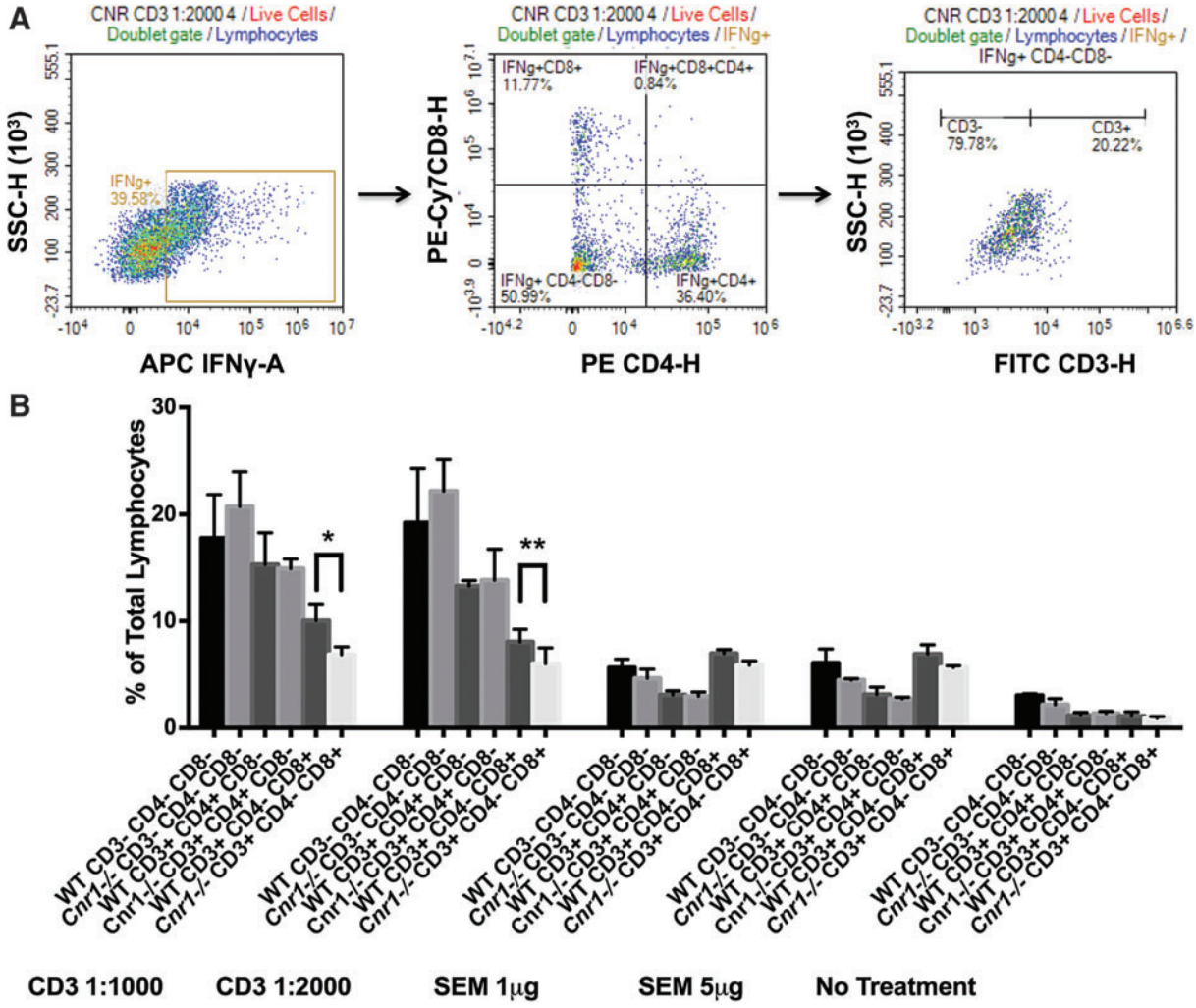

FIG. 7. Analysis of IFN-γ production in anti-CD3/anti-CD28- and SEM-stimulated splenocytes by flow cytometry. IFN-γ production was analyzed by flow cytometry after anti-CD3/anti-CD28 antibody or SEM stimulation of splenocytes from female *Cnr1*$^{-/-}$ and WT mice. IFN-γ producing cells were subdivided based on their CD4, CD8, and CD3 expression by first isolating IFN-γ producing lymphocytes, then determining the expression of CD4 and CD8 on these cells, and finally determining the expression of CD3 within these subpopulations **(A)**. Graph **(B)** represents the percentages of IFN-γ producing cells obtained after an *in vitro* 3-day stimulation of naive splenocytes from a female mouse (this can be used for comparison with the *ex vivo* 3-day restimulation of splenocytes from the female EAE mice in Fig. 6B). Analysis of various cell types from these stimulations revealed a significantly lower percentage of $CD3^+CD4^-CD8^+$IFN-γ^+ cells in *Cnr1*$^{-/-}$ compared with WT mice when splenocytes were stimulated with anti-CD3/anti-CD28 antibodies. In addition, in these experiments, $CD3^+$ cells appear to be the predominant source of IFN-γ. Statistical analysis was performed using two-way ANOVA followed by Sidak's *post hoc* test. Bars are mean ± SD from quadruplicate wells of one female experiment. *$p < 0.05$, **$p < 0.01$ differences between WT and *Cnr1*$^{-/-}$. Color images are available online.

which regions within the lumbosacral spinal cord differed between *Cnr1*$^{-/-}$ mice and their WT littermates. Differences seen in sections 2, 3, and 4 are important since these sections represent the lumbosacral intumescence, the region of the spinal cord where the nerves for the hindlimbs branch off. Higher histologic scores for these sections could reasonably result in an increase in dysfunction in the hindlimbs and worse clinical disease. We also found that our histologic scoring system was more sensitive for detecting disease than clinical scores. This is shown in Figure 3B, in which some of the mice with a clinical score of 0 received a histologic score >0. One of the major challenges associated with the EAE model is finding a consistent method to correlate the commonly used clinical scoring systems with histologic disease.[10,15,16] This new scoring system is designed to specifically account for the complex distribution of lesions found in the spinal cords of EAE mice, and simplifies the quantification of these lesions into a scoring system that can be easily analyzed using a Mann–Whittney *U* test and correlated to clinical disease. Compared with the previously reported methods of scoring histologic disease, our method requires less expertise to use, implements less complex staining techniques, and preserves the tissues for later use; however, it should be noted that the other scoring methods do account for more pathologic features, such as pial versus parenchymal distribution of cells, compared with our method.[31,32] To validate the scoring system, we generated both a total histologic score and a total lesion area for each spinal cord, and correlated these to the clinical score for each mouse. Analysis of the lesion area showed only a slight increase in the r^2 value compared with the histologic scoring system, which shows that either method would be reasonable for confirming clinical disease. These results show that our method of histologic scoring is a relatively simple way to validate clinical scores in EAE mice.

Another method commonly used for analyzing neuroinflammation in the EAE model is by flow cytometry of cells obtained from homogenizing the spinal cord.[33,34] While this is an undeniably valid way to analyze immune infiltrates, our model does have some advantages over this method. One of the major advantages is that our scoring system allows for analysis of lesion distribution along the spinal cord, and preserves the tissues for future histologic stains. When flow cytometry is used to analyze neuroinflammation, the entire spinal cord is used, which does not show distribution over the spinal cord, and if further information is required, the entire study must be repeated. It is our hope that this method will provide researchers who utilize the EAE model with another tool to validate clinical differences seen in the model, without needing access to anything more than a microscope and the reagents for an H&E stain. Moreover, the preservation of tissues will allow researchers to revisit previous studies with more immunohistochemical techniques to collect more data without the need to perform additional studies. One final note that should be made about this new scoring system is that it might also be able to detect differences in cell function within the spinal cord. For example, if it is used in a study in which the treatment disrupts the function of cells within the spinal cord lesions, but does not alter the migration of cells to the spinal cord, the correlation between histological score and clinical score might be lower in the treated group.

In addition to our examination of neuroinflammation, we also measured IFN-γ and IL-17A in the peripheral immune response. These two cytokines are commonly used end-points in the EAE model because Th1 and Th17 cells have been shown to be important in the pathogenesis of EAE and MS.[9–14] Analysis of IFN-γ and IL-17A concentrations within the supernatants of MOG_{35-55}-restimulated splenocytes and serum obtained from our EAE mice showed increased levels of IFN-γ in the supernatants of restimulated splenocytes from *Cnr1*$^{-/-}$ mice compared with their WT littermates. These results are consistent with those found in another study, which showed that treatment of EAE mice with SR141716A increased IFN-γ production in MOG_{35-55}-restimulated splenocytes, along with other proinflammatory cytokines such as IL-17A, IL-1β, IL-6, and TNF-α.[35] It is unclear why we did not see an increase in IL-17A; however, their use of the CB_1 receptor antagonist SR141716A versus our use of the CB_1 knockout mice might have caused this inconsistency.

Since the restimulation method used in these EAE studies relies on the uptake of MOG_{35-55} by APCs and presentation to T cells, we further tested the T cell-specific IFN-γ responses of *Cnr1*$^{-/-}$ and WT mice with naive splenocytes in response to two methods of T cell stimulation *in vitro*: anti-CD3/anti-CD28 antibodies and the *S. aureus* SAg SEM. Anti-CD3/anti-CD28 antibodies act directly on the T cell receptor (TCR) CD3ε subunit and on the CD28 costimulatory molecule to invoke a strong T cell-specific response, which includes increased IFN-γ production. Conversely, the stimulation of T cells with SEM, a pyrogenic toxin SAg, is dependent on cross bridging of the TCR to

MHC class II molecules on APC.[36] Thus, by including both methods, we were first able to assess the ability of T cells alone to produce IFN-γ and then assess their ability to produce IFN-γ in an APC-dependent manner. In addition, since there are differences in the number of women and men affected by MS,[3,4] we included both female and male mice in these stimulations to identify potential sex-specific differences associated with cannabinoid receptor deletion, although we did not detect any notable differences in the IFN-γ responses of splenocytes obtained from female and male mice. Interestingly, when anti-CD3/anti-CD28 antibodies were used, a very robust IFN-γ response was seen in WT and *Cnr1*$^{-/-}$ mice, but the WT mice had nearly a twofold higher level of IFN-γ in the supernatants compared with the *Cnr1*$^{-/-}$ mice. In contrast, when SEM was used to stimulate the splenocytes, lower concentrations of IFN-γ were observed compared with the anti-CD3/anti-CD28 stimulations, and although WT mice generally had higher levels of IFN-γ production compared with the CB_1-deficient mice, the difference was less significant than observed with anti-CD3/anti-CD28 stimulations. The reason for this discrepancy is unclear, although it may be due to the relative strength of the stimulation caused by the anti-CD3/anti-CD28 antibodies compared with SEM. If this is true, then it could mean that the inability of *Cnr1*$^{-/-}$ splenocytes to produce IFN-γ becomes more pronounced at higher levels of stimulation. Since the results from the *in vitro* stimulations contradicted the results found from the *ex vivo* restimulation of splenocytes in our EAE studies, we used flow cytometry to determine the sources of IFN-γ under both conditions.

The results from our flow cytometry did not show a difference in the percentage of IFN-γ producing cells between *Cnr1*$^{-/-}$ and WT mice under most conditions, with the one exception being the anti-CD3/anti-CD28-stimulated $CD3^+CD8^+$ cells; however, it did reveal that the major source of the IFN-γ in our EAE studies was a $CD3^-CD4^-CD8^-$ cell population, and the major source of IFN-γ from the T cell-specific stimulations was the $CD3^+CD4^+$ and $CD3^+CD8^+$ populations. Based on these results, it is clear that IFN-γ production in the EAE model was enhanced in the peripheral immune system of *Cnr1*$^{-/-}$ mice compared with WT mice, however, the increased IFN-γ production *ex vivo* is not explained by an increase in IFN-γ production by T cells specifically. Furthermore, since our flow cytometry analysis showed this cell population to be a $CD3^-$ population, we can rule out NKT cells and $\gamma\delta$ T cells as the source of IFN-γ. These results suggest that NK cells or APCs could be sources of IFN-γ since they are both $CD3^-$. Given the fact that only MOG_{35-55} peptide was added to the cultures to stimulate an antigen-specific response, the data suggest that the major source of IFN-γ in the *ex vivo* cultures was likely either a macrophage or dendritic cell population, which would further suggest that the inflammatory potential of these APCs are enhanced in the *Cnr1*$^{-/-}$ mice. This is supported by the study by Lou et al., in which they examined the effects of SR141716A on IFN-γ production in T cells from EAE mice and BV-2 microglia. When this group examined the effects of SR141716A on T cells from EAE mice, they did so by flow cytometry, much like the present study, and while they did find a significant increase in the overall percentage of $CD4^+$IFN-γ^+ cells with SR141716A treatment, the total percentage of $CD4^+$IFN-γ^+ cells was less than 5% with the difference found between groups only being about 1% of cells.[30] These numbers are very similar to those found in the present study for percentages of $CD4^+$IFN-γ^+ cells, despite the fact that they specifically isolated $CD4^+$ T cells and cocultured them with BV-2 microglial cells before flow cytometry. In addition, when this group examined IFN-γ production by BV-2 microglial cells by ELISA of supernatants from culture, they found that SR141716A-treated microglia had significantly more IFN-γ production compared with those not treated with SR141716A.[30] While further studies need to be done to confirm the source of IFN-γ in our study, the similarities between microglial cells and macrophages strongly support macrophages as a major source of IFN-γ within the peripheral immune response of the EAE model and that CB_1-deficient mice may have a higher level of IFN-γ production in these cells. It should also be noted that when mononuclear cells from the spleens of EAE mice were cultured in the presence of MOG_{35-55} and MBP_{68-86}, an increase in IFN-γ production was also noted by Lou et al., however, in that study no determination of cell types was made.[30]

Conclusion

In this study, we examined differences in the peripheral and neuroimmune response of WT and *Cnr1*$^{-/-}$ mice in the EAE model. The disease progression of EAE seen in this study resembled those seen in previous studies with *Cnr1*$^{-/-}$ mice developing more severe disease compared with WT littermates, although there are some key differences between our work and that done in ABH mice as noted above.[16,17,30] In addition,

we introduced a novel method of scoring histologic disease that confirmed the differences seen in the clinical progression between these two groups of mice. Through our examination of IFN-γ production in *Cnr1*$^{-/-}$ and WT mice under various experimental conditions, we found that CB_1-deficient mice had both increased and decreased production of IFN-γ, which was highly dependent on which cells are stimulated. More specifically, when the CD3$^-$ populations dominated IFN-γ production in our EAE studies, *Cnr1*$^{-/-}$ mice produced higher levels of IFN-γ and when T cells dominated IFN-γ production in our T cell-specific stimulation cultures, WT mice had higher levels of IFN-γ. Further studies must be done to better understand which cells in the CD3$^-$ population are contributing to the increased production of IFN-γ during EAE, however, as we have noted, it is likely that dendritic cells or macrophages are responsible for the increase. These results represent an important step in understanding the complex mechanism of the CB_1 receptor in different cell types, and under different stimulation conditions. Moreover, these results show that the effects elicited by the therapeutic targeting of the endocannabinoid system, and more specifically the CB_1 receptor, may be dependent on the status of the immune system at the time of treatment.

Acknowledgments

The authors recognize Dr. Graham Rosser for image formatting, Dr. Keun Seok Seo and Dr. Nogi Park for providing SEM, and Dr. Brittany Szafran for management of the *Cnr1*$^{-/-}$ breeding colony.

Author Disclosure Statement

No competing financial interests exist for any of the authors.

Funding Information

Studies were funded by the Mississippi State University College of Veterinary Medicine.

References

1. Browne P, Chandraratna D, Angood C, et al. Atlas of Multiple Sclerosis 2013: a growing global problem with widespread inequity. Neurology. 2014;83:1022–1024.
2. Dobson R, Giovannoni G. Multiple sclerosis—a review. Eur J Neurol. 2019; 26:27–40.
3. Ramagopalan SV, Byrnes JK, Orton SM, et al. Sex ratio of multiple sclerosis and clinical phenotype. Eur J Neurol. 2010;17:634–637.
4. Alonso A, Jick SS, Olek MJ, et al. Incidence of multiple sclerosis in the United Kingdom: findings from a population-based cohort. J Neurol. 2007;254:1736–1741.
5. Tintore M, Vidal-Jordana A, Sastre-Garriga J. Treatment of multiple sclerosis—success from bench to bedside. Nat Rev Neurol, 2019;15:53–58.
6. Howlett AC, Shim JY. Cannabinoid receptors and signal transduction, in Madame Curie Bioscience Database [Internet]. 2000–2013, Landes Bioscience: Austin, TX.
7. Turcotte C, Blanchet MR, Laviolette M, et al. The CB2 receptor and its role as a regulator of inflammation. Cell Mol Life Sci. 2016;73:4449–4470.
8. Dendrou CA, Fugger L, Friese MA. Immunopathology of multiple sclerosis. Nat Rev Immunol. 2015;15:545–558.
9. Kozela E, Juknat A, Kaushansky N, et al. Cannabinoids decrease the th17 inflammatory autoimmune phenotype. J Neuroimmune Pharmacol. 2013; 8:1265–1276.
10. Giacoppo S, Pollastro F, Grassi G, et al. Target regulation of PI3K/Akt/mTOR pathway by cannabidiol in treatment of experimental multiple sclerosis. Fitoterapia. 2017;116:77–84.
11. Fletcher JM, Lalor SJ, Sweeney CM, et al. T cells in multiple sclerosis and experimental autoimmune encephalomyelitis. Clin Exp Immunol. 2010; 162:1–11.
12. Brucklacher-Waldert V, Stuerner K, Kolster M, et al. Phenotypical and functional characterization of T helper 17 cells in multiple sclerosis. Brain. 2009;132(Pt 12):3329–3341.
13. Langrish CL, Chen Y, Blumenschein WM, et al. IL-23 drives a pathogenic T cell population that induces autoimmune inflammation. J Exp Med. 2005; 201:233–240.
14. Tzartos JS, Friese MA, Craner MJ, et al. Interleukin-17 production in central nervous system-infiltrating T cells and glial cells is associated with active disease in multiple sclerosis. Am J Pathol. 2008;172:146–155.
15. Elliott DM, Singh N, Nagarkatti M, et al. Cannabidiol attenuates experimental autoimmune encephalomyelitis model of multiple sclerosis through induction of myeloid-derived suppressor cells. Front Immunol. 2018;9:1782.
16. Pryce G, Ahmed Z, Hankey DJ, et al. Cannabinoids inhibit neurodegeneration in models of multiple sclerosis. Brain. 2003;126(Pt 10):2191–2202.
17. Maresz K, Pryce G, Ponomarev ED, et al. Direct suppression of CNS autoimmune inflammation via the cannabinoid receptor CB1 on neurons and CB2 on autoreactive T cells. Nat Med. 2007;13:492–497.
18. Pryce G, Baker D. Control of spasticity in a multiple sclerosis model is mediated by CB1, not CB2, cannabinoid receptors. Br J Pharmacol. 2007; 150:519–525.
19. Ameri A. The effects of cannabinoids on the brain. Prog Neurobiol 1999; 58:315–348.
20. Svizenska I, Dubovy P, Sulcova A. Cannabinoid receptors 1 and 2 (CB1 and CB2), their distribution, ligands and functional involvement in nervous system structures—a short review. Pharmacol Biochem Behav. 2008;90: 501–511.
21. Kaminski NE, Abood ME, Kessler FK, et al. Identification of a functionally relevant cannabinoid receptor on mouse spleen cells that is involved in cannabinoid-mediated immune modulation. Mol Pharmacol. 1992;42: 736–742.
22. Galiegue S, Mary S, Marchand J, et al. Expression of central and peripheral cannabinoid receptors in human immune tissues and leukocyte subpopulations. Eur J Biochem. 1995;232:54–61.
23. Sisay S, Pryce G, Jackson SJ, et al. Genetic background can result in a marked or minimal effect of gene knockout (GPR55 and CB2 receptor) in experimental autoimmune encephalomyelitis models of multiple sclerosis. PLoS One. 2013;8:e76907.
24. Al-Ghezi ZZ, Miranda K, Nagarkatti M, et al. Combination of cannabinoids, Delta9- tetrahydrocannabinol and cannabidiol, ameliorates experimental multiple sclerosis by suppressing neuroinflammation through regulation of miRNA-mediated signaling pathways. Front Immunol. 2019;10:1921.
25. Vaney C, Heinzel-Gutenbrunner M, Jobin P, et al. Efficacy, safety and tolerability of an orally administered cannabis extract in the treatment of spasticity in patients with multiple sclerosis: a randomized, double-blind, placebo-controlled, crossover study. Mult Scler. 2004;10:417–424.
26. Zajicek J, Fox P, Sanders H, et al. Cannabinoids for treatment of spasticity and other symptoms related to multiple sclerosis (CAMS study): multicentre randomised placebo-controlled trial. Lancet. 2003;362:1517–1526.
27. Wade DT, Makela P, Robson P, et al. Do cannabis-based medicinal extracts have general or specific effects on symptoms in multiple sclerosis? A double-blind, randomized, placebo-controlled study on 160 patients. Mult Scler. 2004;10:434–441.
28. Collin C, Davies P, Mutiboko IK, et al. Randomized controlled trial of cannabis-based medicine in spasticity caused by multiple sclerosis. Eur J Neurol. 2007;14:290–296.

29. Lorente Fernandez L, Monte Boquet E, Perez-Miralles F, et al. Clinical experiences with cannabinoids in spasticity management in multiple sclerosis. Neurologia. 2014;29:257–260.
30. Lou ZY, Cheng J, Wang XR, et al. The inhibition of CB1 receptor accelerates the onset and development of EAE possibly by regulating microglia/macrophages polarization. J Neuroimmunol. 2018;317:37–44.
31. Goncalves DaSilva A,Yong VW. Matrix metalloproteinase-12 deficiency worsens relapsing-remitting experimental autoimmune encephalomyelitis in association with cytokine and chemokine dysregulation. Am J Pathol. 2009;174:898–909.
32. Sloka S, Metz LM, Hader W, et al. Reduction of microglial activity in a model of multiple sclerosis by dipyridamole. J Neuroinflammation. 2013;10:89.
33. Li YH, Xu F, Thome R, et al. Mdivi-1, a mitochondrial fission inhibitor, modulates T helper cells and suppresses the development of experimental autoimmune encephalomyelitis. J Neuroinflammation. 2019;16:149.
34. Zhou S, Liu G, Guo J, et al. Pro-inflammatory effect of downregulated CD73 expression in EAE astrocytes. Front Cell Neurosci. 2019;13:233.
35. Lou ZY, Zhao CB, Xiao BG. Immunoregulation of experimental autoimmune encephalomyelitis by the selective CB1 receptor antagonist. J Neurosci Res. 2012;90:84–95.
36. Dinges MM, Orwin PM, Schlievert PM. Exotoxins of *Staphylococcus aureus*. Clin Microbiol Rev. 2000;13:16–34, table of contents.

Cite this article as: Nichols JM, Kaplan BLF (2021) The CB_1 receptor differentially regulates IFN-γ production *in vitro* and in experimental autoimmune encephalomyelitis, *Cannabis and Cannabinoid Research* 6:4, 300–314, DOI: 10.1089/can.2020.0046.

Abbreviations Used

2-ME = 2-mercaptoethanol
ANOVA = analysis of variance
APC = antigen presenting cell
AUC = area under the curve
BSA = bovine serum albumin
CBD = cannabidiol
CFA = complete Freund's adjuvant
EAE = experimental autoimmune encephalomyelitis
EDTA = ethylenediaminetetraacetic acid
ELISA = enzyme-linked immunosorbent assay
FCM = flow cytometry media
H&E = hematoxylin and eosin
HKMT = heat-killed Mycobacterium tuberculosis
HRP = horseradish peroxidase
MOG = myelin oligodendrocyte glycoprotein
MS = multiple sclerosis
NIR FVD = Near Infrared Fixable Viability Dye
PBS = phosphate-buffered saline
PBST = PBS containing 0.05% Tween 20
RT = room temperature
SAL = saline
SEM = staphylococcal enterotoxin M
TCR = T cell receptor
THC = Δ^9-tetrahydrocannabinol
WT = wild type